International Journal of Advanced Science and Technology
Vol. 29, No. 06, (2020), pp. 6844-6863

Estımatıon Of Hypersonıc Unsteady And Qausı-Steady Dampıng Derıvatıves For A Delta Wıngs At Large IncıdenceDrives

Renita Sharon Monis[1], Asha Crasta[2], Sher Afghan Khan[3]

[1]*Research Scholar, Mathematics Dept., M.I.T.E, Moodabidri and Sr. Assistant Professor, SMVITM, Bantakal, Karnataka, India*
[2] *Associate Professor, Mathematics Department, M.I.T.E, Moodabidri, Karnataka, India*
[3] *Professor, Department of Mechanical Engineering, Faculty of Engineering, IIUM, Gombak Campus, uala Lumpur, Malaysia*
[1]*renita.maths@sode-edu.in,* [2]*asha@mite.ac.in,* [3]*sakhan@iium.edu.my*

Abstract

This paper presents results of quasi-steady and unsteady damping derivatives of a delta wing whose leading edge is straight. Results are computed for a wide range of Mach numbers and angles of attack. Here the contribution to the damping derivatives due to the rate of change of angle of attack is estimated separately. The results show that with the increase in Mach number, there is a progressive decrease in the damping derivatives for both the cases (i.e., unsteady and quasi-steady). With the further rise in the Mach values, the magnitude of decline has diminished for Mach number M = 10 and above the state of steady-state is achieved. For the entire range of the Mach number, the location of the center of pressure remained unchanged for a fixed value of the flow deflection angle δ. For the lower flow deflection angle of the wing, the magnitude of the damping derivatives is smaller as compared to the higher values of δ. The contribution to the damping derivatives from the rate of change of angle of attack is around 20 percent of the quasi-steady one. The results for flow deflection angles of ten degrees and twenty degrees show a different trend. When we compare the results of the damping derivatives for a fixed pivot position, it is seen that the damping derivatives show different behavior for two different values of the flow deflection angle δ. The steady-state varies for two values of δ. When we look at the damping derivatives at hinge point k = 0.6, the magnitude is small. The steady-state is attained early for quasi-steady in comparison to the unsteady damping derivatives.

Keywords–*Damping derivative, Delta wing, Hypersonic, Straight leading-edge, Pivot position*

1. Introduction

The simulation of the static, as well as the dynamic stability of the aerospace vehicles, is critical before we decide to go for the fabrication of the prototype. At the initial design stage of the aerospace vehicles, knowledge of the stability derivative is of prime importance. Theoretical computation of the stability derivatives gives a fair idea about the performance of aerospace vehicles. Since wind tunnel tests require an enormous amount of cost in model making and wind tunnel tests, therefore designers prefer to do the simulations. Then once a design is almost frozen, only they plan to fabricate the model and conduct the wind tunnel tests. Before the wind tunnel tests, the designer is required to satisfy the geometrical similarity, kinematical similarity, and dynamic similarity. The literature review shows that it is straightforward to achieve geometrical and kinematical similarity. However, the matching of the dynamic similarity parameter is challenging. For instance, when we conduct the wind tunnel tests, the Reynolds number of the wind tunnel section while doing the tests is different when the aerospace vehicle is flying at higher altitude where the air density is low. The Reynolds number is low as compared to the wind tunnel

ISSN: 2005-4238 IJAST

test section Reynolds number. Hence, this is one of the biggest challenges to address if you want to make use of the wind tunnel test results. This paper discusses the computation of damping derivatives for a delta wing with straight leading edges. The delta wing has the edge over conventional rectangular and tapered wing. It is well known that the pressure on the lee side will be negligible as compared to the windward surface as we are dealing with the hypersonic Mach numbers. However, if we are evaluating the damping derivative at supersonic Mach numbers, the pressure on the lee surface can not be ignored as it will be considerable. In this paper, we limit our study at Mach five and above; hence the lee pressure is not taken into consideration.

A 2-D hypersonic similitude at large incidence along with piston theory, including Light hill's [1] and Mile's [2], has been developed by Ghosh [3]. For the windward surface theory of order of $\phi^{2,}$ where ¢ is the angle between the attached shock and the plane approximation is applied by Ghosh and Mistry [4].

Similitude and two similarity parameters were obtained by Ghosh [5] for shock attached oscillating delta wings at large incidence. In the present analysis, this similitude has been extended to shock attached delta wings with straight leading edges at large incidence. The lee surface is assumed to be zero.

The problem of stability of an oscillating flat plate wing in supersonic/hypersonic flow of arbitrary plan form shape placed at a certain mean angle of attack studied by Hui et al. [9] by applying strip-theory. It is assumed that at each spanwise station, the flow will be locally 2-D with the shock attached. They obtained stability derivatives of a wing of arbitrary plan form in closed form. It is not valid for detached shock flow and also in the region where vortex roll-ups or separation becomes significant. Its accuracy improves with an increase in free stream Mach number and becomes exact in the Newtonian limit where fluid particles do not interact with each other, and it becomes genuinely 2-D locally. Ghosh has extended the large deflection similitude to non-slender cones, quasi cones, and also for wings provided the shock wave is attached with the leading edge of wedge/cone/delta wings.

Crasta and Khan [11]-[20] have studied the effect of angle of incidence on pitching derivatives and roll damping derivatives of a delta wing with curved leading edges. Aerodynamic variables are computed for a wing with variable-sweep angles by Crasta& S. A. Khan by evaluating the effectiveness of the flow deflection angle. Monis et.al.[21-26] estimated for low as well as for extraordinary Mach M the stability derivatives in pitch and damping.

When we consider the various strips at different locations along the span of the wing, it becomes independent of the strips. Hence, with these two assumptions, the three-dimensional flow is reduced to a one-dimensional flow or piston motions. Here, results are obtained from the second-order shock-expansion theory by getting the piston theory.

The overall stability of the wedge/wing is assessed based on the moment derivatives due to the pitch rate as well as incident rate are evaluated. The Ghosh [8] hypersonic similitude along with the Crasta& Khan [11]-[20] theory is integrated with the strip theory to obtain the unsteady moment derivative for a wing with the straight leading edge. Crasta and Khan developed a theory to evaluate the stability derivatives in pitch, which does not cater to the unsteady effect as the theory developed by them is a quasi-steady one. This paper computes the unsteady damping derivative and then evaluates quasi-steady damping derivative, and by subtracting from the previous will give the damping derivative due to the rate of change of angle of attack alone. We have calculated $-C_{m\dot{\alpha}}$ that is the damping derivative due to the rate of change of angle of attack by using the expression,

$$-C_{m\dot{\alpha}} = -C_{m\dot{\theta}} - (-C_{mq}).$$

2. Analysıs:

The pitching moment per unit span about the pivot x = x_0 due to the only lower surface is,

$$\overline{M} = \int_0^L (x - kL)\bar{P}_p dx$$

$$-\frac{\partial \bar{M}}{\partial \dot{\theta}} = \int_0^L (x - kL)\frac{\partial \bar{P}_p}{\partial \dot{\theta}} dx$$

$$-\frac{\partial \bar{M}}{\partial \dot{\theta}} = \int_0^L (x - kL)\rho_2 a_2 u_\infty \left(\frac{c_2 x}{u_\infty} + \frac{c_3 L}{u_\infty}\right) dx$$

For the windward side, the equation is

$$-\frac{\partial M}{\partial \dot{\theta}} = \rho_2 a_2 L^3 \left[c_2\left(\frac{1}{3} - \frac{k}{2}\right) + c_3\left(\frac{1}{2} - k\right) \right]$$

On the expansion side of the flat plate, the flow turns through a Prandtl-Meyer expansion at the leading edge to become parallel to the upper surface. First, Mach number M_θ downstream of the expansion fan is determined first.

At zero angle of attack, flat plate oscillating in a stream of Mach number $M_{\theta,}$ it is assumed that pressure perturbation is the same. Due to this approach, the oscillation of the expansion fan due to the flat plate oscillation is not considered. It is worth noting that the upper surface is at a much lower pressure than the windward side. Contribution to damping at large Mach numbers is negligible as compared to the windward side of the wing.

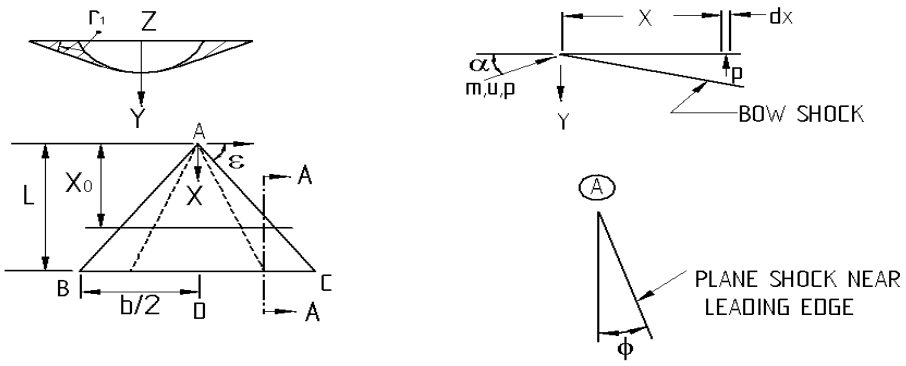

Fig. 1 Different views of the Delta Wing

$$V_p = \frac{u_\theta}{\cos\mu_\theta} + \frac{(x-kL)\dot{\theta}}{\cos\mu_\theta}$$

Piston Mach Number

$$M_p = \frac{v_p}{a_\theta} = \frac{M_\theta \theta}{\cos\mu_\theta} + \frac{(x-kL)\dot{\theta}}{a_\theta \cos\mu_\theta} \qquad \ldots\ldots\ldots\ldots\ldots\ldots\ldots\ldots\ldots\ldots\ldots\ldots(1)$$

M_θ is the Mach number downstream of the expansion fan, a_θ is the sonic velocity & μ_θ is the Mach angle downstream of Prandtl- Mayer expansion.

The isentropic expression for pressure ratio is given by

$$\frac{p_p}{P_\theta} = \left(1 - \frac{\gamma-1}{2} M_p\right)^{\frac{2\gamma}{\gamma-1}}$$

As θ and $\dot{\theta}$ tend to zero, the equation for the acoustic expression

$$\frac{P_p}{P_\theta} \approx (1 - \gamma M_P)$$

Pitching moment,

$$\bar{M} = \int_0^L (x-kL) P_p \, dx = \int_0^L (x-kL) P_\theta (1-\gamma M_P) \, dx$$

$$-\frac{\partial \bar{M}}{\partial \dot{\theta}} = \int_0^L (x-kL) P_\theta (-\gamma) \frac{\partial M_p}{\partial \dot{\theta}} \, dx$$

From equation (1)

ISSN: 2005-4238 IJAST

$$-\frac{\partial \bar{M}}{\partial \dot{\theta}} = -\int_0^L (x-kL) P_\theta(-\gamma) \frac{(x-kL)}{a_\theta \cos \mu_\theta} dx$$

$$-C_{m_{\dot{\theta}}} = \frac{4}{\rho_\infty u_\infty b L^3}\left[-\frac{\partial \bar{M}}{\partial \dot{\theta}}\right]$$

$$-C_{m_{\dot{\theta}}} = \frac{4\rho_2 a_2}{\rho_\infty u_\infty} \frac{1}{(\cot\varepsilon - \frac{4A_H}{\pi})} \left[\begin{array}{l} c_2[(\frac{1}{8}-\frac{k}{6})\cot\varepsilon - \frac{A_F}{4\pi} - \frac{A_H}{2\pi} - \frac{2A_H}{\pi^3} + \frac{k(A_H + \frac{A_F}{2})}{\pi}] + \\ C_4[(\frac{k}{2} - \frac{k^2}{2} - \frac{1}{8})\cot\varepsilon - \frac{3A_F}{4\pi} + \frac{A_H}{2\pi} - \frac{6A_H}{\pi^3} + \frac{k}{\pi}(\frac{3A_F}{2} - A_H) + 2k^2 \frac{A_H}{\pi}] \end{array}\right] \quad ....(1)$$

When

$A_H = 0, A_F = 0$

$$-C_{m_{\dot{\theta}}} = \frac{4\rho_2 a_2}{\rho_\infty u_\infty}\left[c_2(\frac{1}{8}-\frac{k}{6}) + C_4(\frac{k}{2} - \frac{k^2}{2} - \frac{1}{8})\right]$$

Khan has obtained -C_{mq}(by taking only the windward surface into account)as,

$$-C_{mq} = \frac{\sin\alpha_0 F(s_1)}{\cos^2\phi(\cot\varepsilon - \frac{4A_H}{\pi})}\left[(k^2 - \frac{4}{3}k + \frac{1}{2})\cot\varepsilon - \frac{1}{\pi}((2k-1)A_F + 2A_H(2k^2 - 2k + 1 - \frac{4}{\pi^2}))\right]$$

….(2)

The Effect of Leeward surface can be taken into account by using the strip theory in combination with equation $-\frac{\partial \bar{M}}{\partial q}\Big|_{\alpha=\alpha_0, q\to 0} = \frac{\gamma p_\theta L^3}{a_\theta \cos\mu_\theta}\left[\frac{1}{3} - k + k^2\right]$

We get $-C_{mq}$for the leeward surface as,

$$-C_{mq} = 2\frac{P_\theta}{P_\infty}\frac{a_\infty}{a_\theta}\frac{M_\theta}{M_\infty}\frac{1}{\sqrt{M_\theta{}^2 - 1}}\frac{1}{(\cot\varepsilon - \frac{4A_H}{\pi})}[(\frac{1}{2} - \frac{4k}{3} + k^2)\cot\varepsilon + \frac{2A_H}{\pi}(\frac{4}{\pi^2} - 1) + \frac{2k}{\pi}(2A_H) - \frac{4A_H k^2}{\pi}]$$

The above value should be added to the equation (2) to obtain $-C_{mq.}$

But in this case, we have ignored the expansion term,

So, $-C_{mq}$ for $A_H=0$, $A_F=0$ is,

$$-C_{mq} = \frac{\sin\alpha_0 F(s_1)}{\cos^2\phi}\left[(k^2 - \frac{4}{3}k + \frac{1}{2})\right]$$

Thus we calculate the incident rate-$C_{m\dot{\alpha}}$ for $A_F = 0$, and $A_H = 0$.

$$-C_{m\dot{\alpha}} = -C_{m\dot{\theta}} - (-C_{mq})$$

3. Results and Discussions:

The above expressions for damping derivatives for a fully unsteady case, quasi-steady case, and the contribution of the damping derivatives due to the rate of change of angle of attack alone are computed and shown graphically in this section. Even though the expressions are obtained for a delta wing with curved leading edges, but the results are shown only for the straight leading edge. The results for damping derivatives with straight leading are accomplished by equating the amplitude of the full, and half-sine wave is equal to zero. The contribution of the damping derivatives, due to the angle of incidence, plays a vital role during the design, to arrive at the maximum possible angle of attack that can be used for the wing as well as the control surfaces without compromising on the stability of the aerospace vehicles as well as the structural integrity. Fig. 2 shows the damping derivatives for an unsteady and quasi-steady case at Mach M = 5, and flow deflection angle $\delta = 20^0$. We know that the quasi-steady damping derivative takes in to account the rate of pitch alone and not the rate of change of angle of attack.

In contrast, the fully unsteady damping derivative not only accounts for pitch rate but also for the rate of change of angle of attack.The variation in the damping derivatives between unsteady and quasi-steady is in the range from seventeen percent, twenty-one percent, twenty-seven percent, twenty-five percent, one percent to minus five percent. These results clearly indicate that the magnitude of the damping derivative obtained using the unsteady theory is more than the one evaluated by the quasi-steady theory.

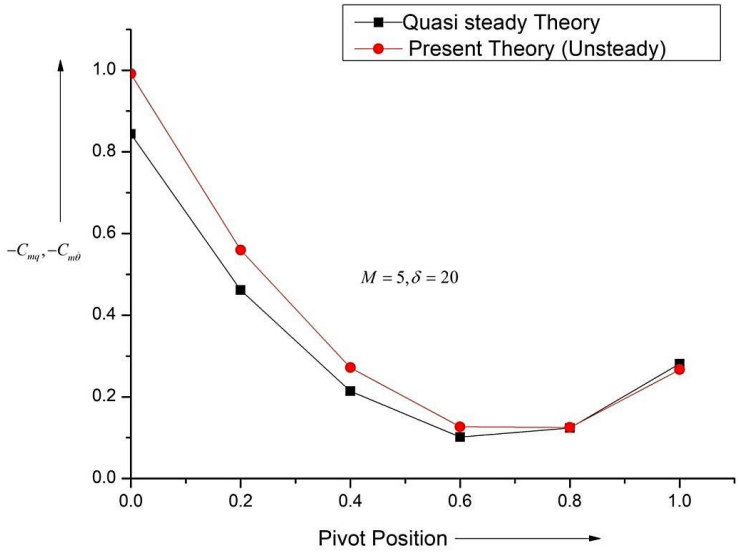

Fig. 2 Unsteady and quasi-steady damping derivative with the pivot position

These results were expected as results with quasi-steady theory does not include the rate of change of the angle of incidence impact during the flight. The results also show that the magnitude of the stability

derivative in damping initially takes relatively high value when it is considered at the pivot location h = 0. As we move downstream, there is a continuous decrease in the magnitude of the derivatives. The reduction in the results is attributed to the decline in the values of the pivot position from the center of pressure. Here the location of the center of pressure is fixed for a given Mach number and the flow deflection angle.

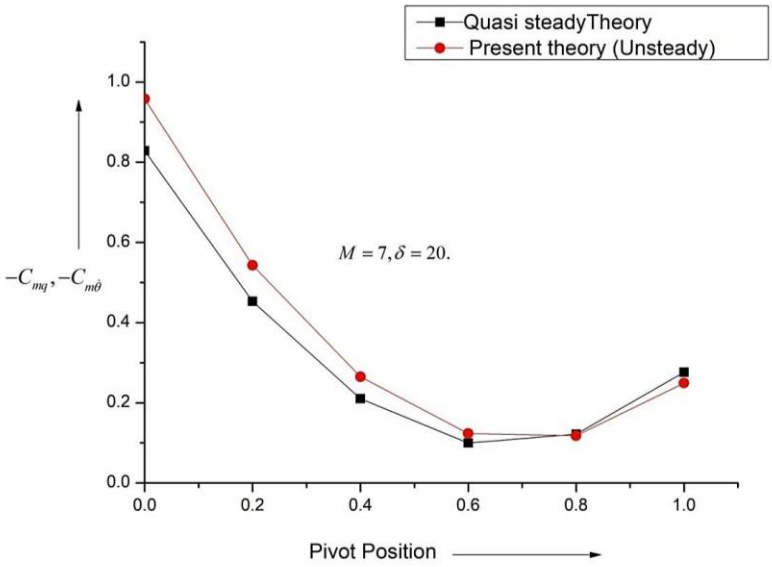

Fig. 3 Unsteady and quasi-steady damping derivative with the pivot position

Figure 3 presents the results for Mach 7, keeping all other parameters the same. It is seen that due to the reduction in the Mach number, there is a marginal decrease in the values of the damping derivatives, and this decrease is uniform for both unsteady and quasi-steady. The variations in the numerical values start from sixteen percent at the pivot position h = 0 then keeps on increasing to twenty percent, twenty-six percent till h = 0.4. Then again, it starts declining to twenty-four percent minus three percent to minus ten percent. In this figure, the effect of the increase in the Mach number is seen.

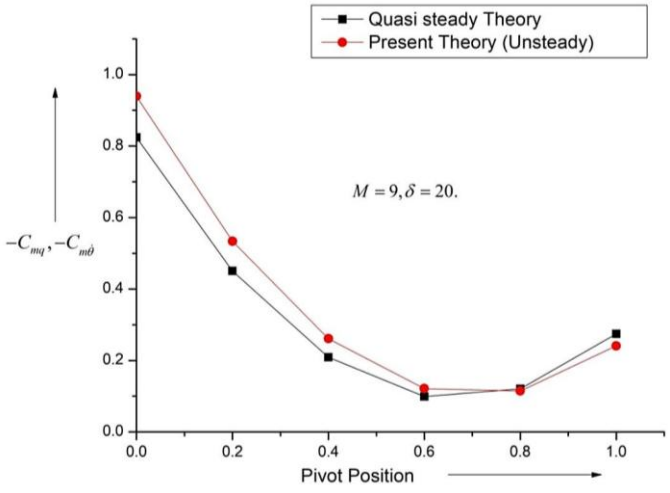

Fig. 4 Unsteady and quasi-steady damping derivative with the pivot position

ISSN: 2005-4238 IJAST

Figure 4 shows the results for Mach M = 9. With a further increase in the inertia levels, there is a further decrease in the damping derivatives. In all these cases, the center of pressure remained at a pivot position of 0.6. The discrepancy between the unsteady and quasi-steady damping derivatives is fourteen percent at h = 0, eighteen percent, twenty-five percent, and twenty-three percent at h = 0.2, 0.4, and 0.6. When we further move downstream, there is a reversal in the trend. The unsteady derivatives, which large in magnitude from h = 0 to 0.6, for the pivot position beyond the center of pressure reversal of the direction, take place. For the last two pivot positions, these values are minus five and twelve percent.

Figure 5 shows the results for Mach M = 12. In this case, there is a further increase in the inertia levels; there is a further decrease in the damping derivatives. The discrepancy between the unsteady and quasi-steady damping derivatives is fourteen percent at h = 0, thirteen percent, seventeen percent, and twenty-four percent at h = 0.2, 0.4, and 0.6. When we further move downstream, there is a reversal in the trend. The unsteady derivatives, which large in magnitude from h = 0 to 0.6, for the pivot position beyond the center of pressure reversal of the direction, take place. For the last two pivot positions, these values are minus seven and fourteen percent.

Figure 6 shows the results for Mach M = 15. With a further increase in the inertia levels, there is a marginal decrease in the damping derivatives. In all these cases, the center of pressure remained at a pivot position of 0.6. The discrepancy between the unsteady and quasi-steady damping derivatives is twelve percent at h = 0, sixteen percent, twenty-three percent, and twenty-one percent at h = 0.2, 0.4, and 0.6. When we further move downstream, there is a reversal in the trend. The unsteady derivatives, which large in magnitude from h = 0 to 0.6, for the pivot position beyond the center of pressure reversal of the direction, take place. For the last two pivot positions, these values are minus eight and fifteen percent.

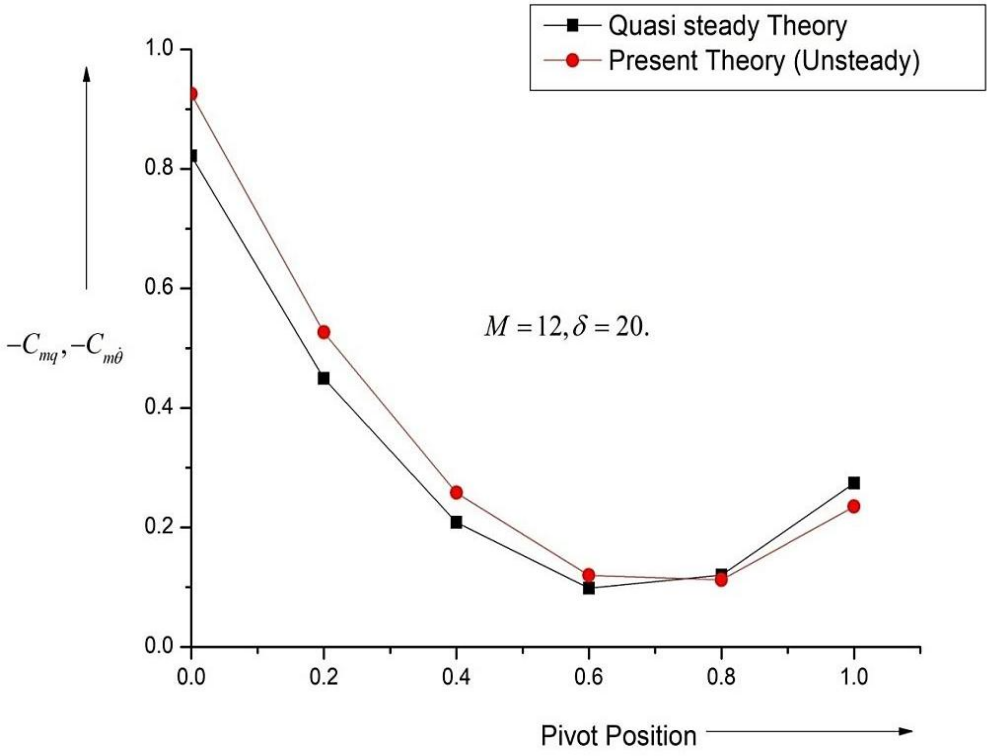

Fig. 5 Unsteady and quasi-steady damping derivative with the pivot position

ISSN: 2005-4238 IJAST

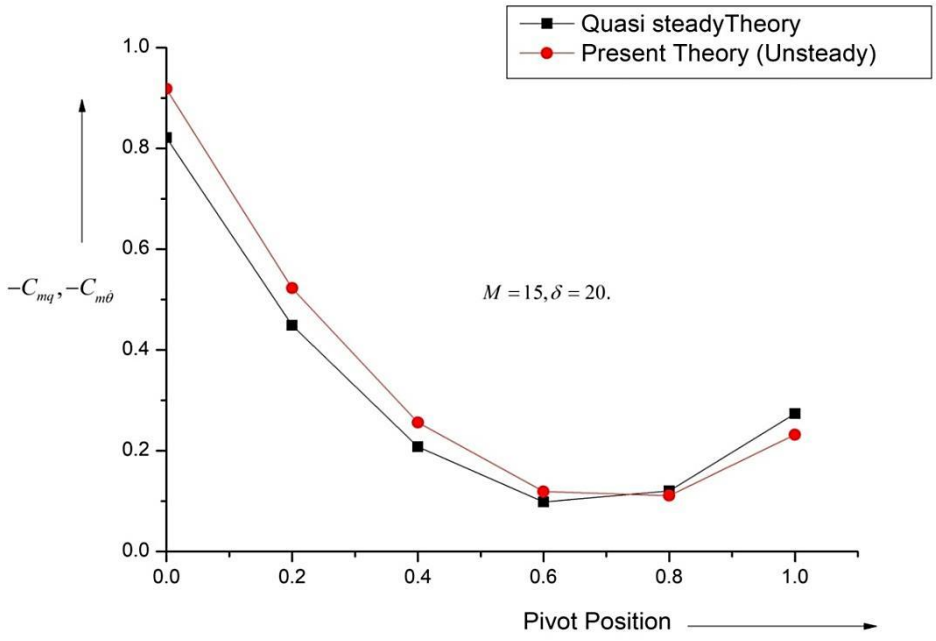

Fig. 6 Unsteady and quasi-steady damping derivative with the pivot position

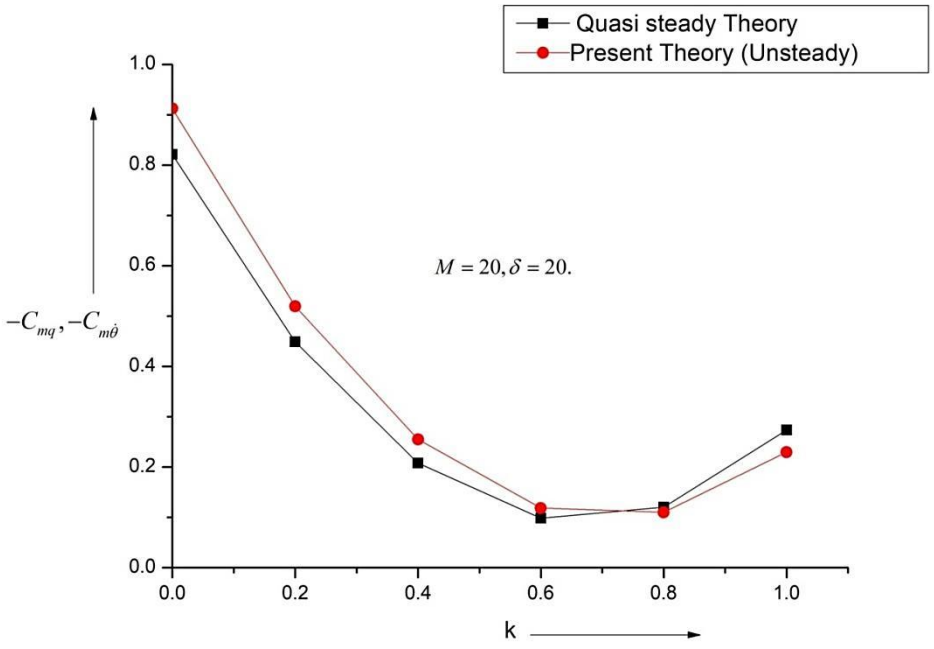

Fig. 7 Unsteady and quasi-steady damping derivative with the pivot position

Figure 7 presents the results of damping derivatives and the comparative numerical values for unsteady and quasi-steady at Mach M = 20. Mach M = 20 is the highest inertia level of the present study. When we compare the results with the previous Mach number M = 15, the results show that the numerical values

ISSN: 2005-4238 IJAST

are in the same range. The results have achieved the steady-state; this also confirms the Mach number independence principle.

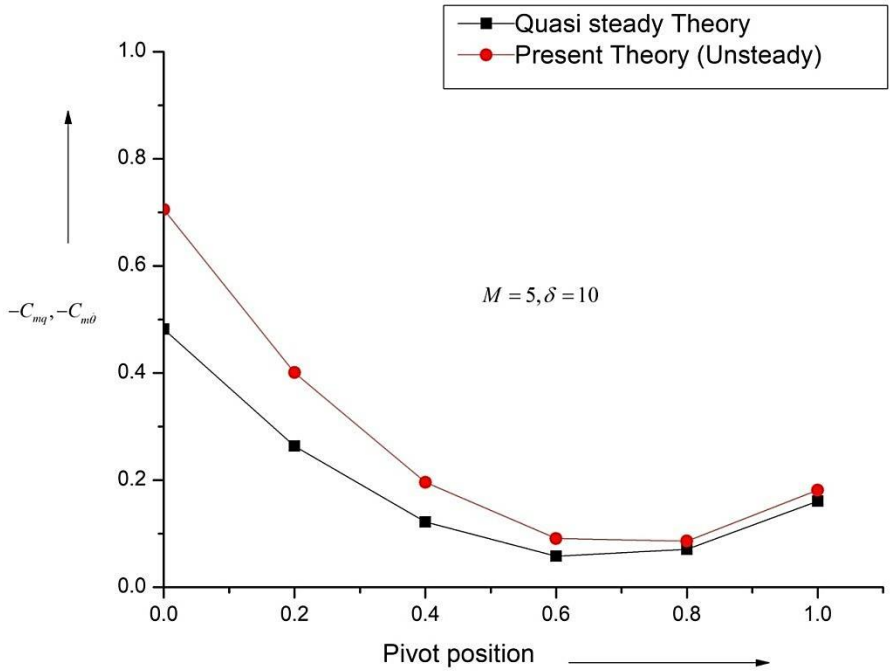

Fig. 8 Unsteady and quasi-steady damping derivative with the pivot position

Figure 8 shows the results for a lower value of the flow deflection (i.e., $\delta = 10^0$) at the lowest value of inertia level (i.e., M = 5). The outcomes for this value of $\delta = 10$ degrees are different when we compare them with $\delta = 20$ degrees. Figure 8 shows a wide range of variations in the magnitude of the values. The discrepancies in the data are forty-six percent, fifty-two percent, sixty percent, fifty-seven percent, twenty-two percent, and thirteen percent for h = 0, 0.2, 0.4, 0.6, 0.8, and 1. In view of the above results and the discussion on the damping derivative for a large flow deflection angle, the trend is different. It is evident that for the pivot position in the range from h= 0. 4 to 0.6, a reversal in the trend which was taking place is missing in this case. That means the numerical values of the damping derivatives for quasi-steady cases, which was lower in magnitude, becomes more considerable for the pivot position in the neighborhood of the center of pressure. It is also seen that the damping derivatives are higher for the entire range of the pivot positions. Results also indicate that the discrepancy in the numerical values is large for the initial pivot position, and it continues to decrease with the movement of the pivot position. This drastic change is due to a reduction in the planform area of the wing at lower values of the δ, and a decrease in the flow deflection angle will have a different flow field on the surface of the wing.

ISSN: 2005-4238 IJAST

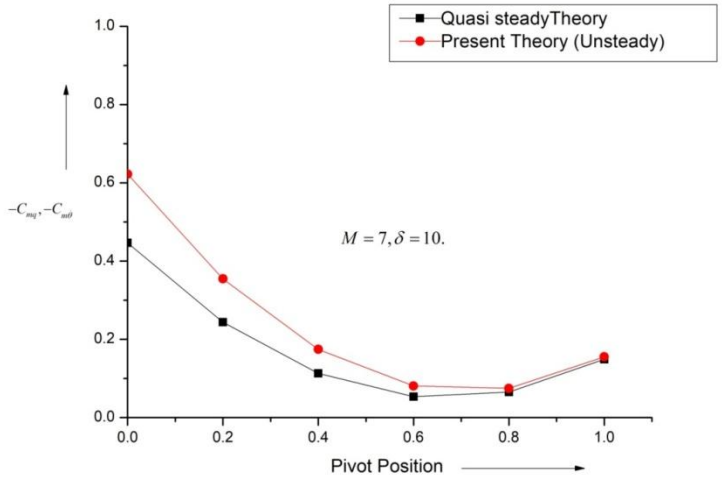

Fig. 9 Unsteady and quasi-steady damping derivative with the pivot position

Similar results are seen for Mach M = 7 in Figure 9 for a lower value of the flow deflection (i.e., $\delta = 10^0$). Figure 9 shows a similarly wide range of variations in the magnitude of the values of the stability derivatives. The only exception, in this case, is that level of inertia has marginally increased as compared to the previous case. The discrepancies in the data are thirty-nine percent, forty-five percent, fifty-four percent, fifty-one percent, fourteen percent, and four percent for h = 0, 0.2, 0.4, 0.6, 0.8, and 1 because of the above results and the discussion on the damping derivative for a large flow deflection angle. The outcomes reiterate that for the pivot positions ranging from h= 0. 4 to 0.6, a reversal in the trend does not take place. That means the numerical values of the damping derivatives for quasi-steady cases, which was lower in magnitude, becomes more considerable for the pivot position in the neighborhood of the center of pressure. This drastic change is due to a reduction in the planform area of the wing at lower values of the δ, and a decrease in the flow deflection angle will have a different flow field on the surface of the wing.

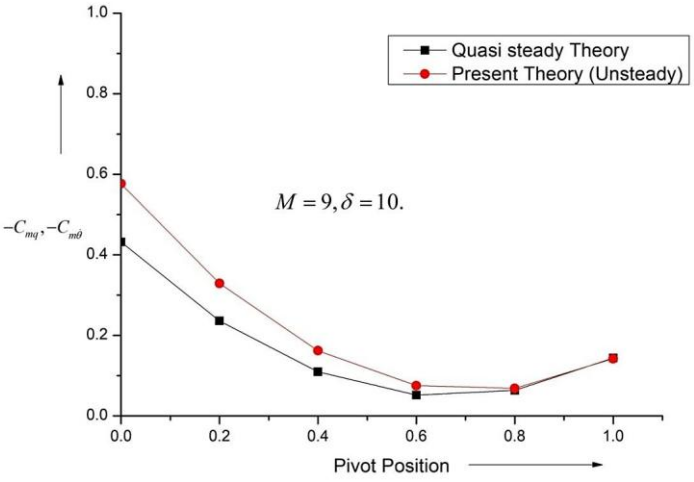

Fig. 10 Unsteady and quasi-steady damping derivative with the pivot position

Figure 10 shows the results at the more considerable value of inertia level (i.e., M = 9). The outcomes for this value of δ = 10 degrees are now marginally different when we compare them with δ = 20 degrees. Figure 10 shows a wide range of variations in the magnitude of the values. The discrepancies in the data are thirty-three percent, thirty-nine percent, forty-eight percent, forty-five percent, eight percent, and minus one percent for h = 0, 0.2, 0.4, 0.6, 0.8, and 1. It is evident that for the pivot position of h = 0.8, a reversal in the trend is taking place.This implies that the trends which were seen for δ = 20 degrees have surfaced once again once the Mach number has increased considerably. It is also noticed that the damping derivatives are lower for the entire range of the pivot positions. This drastic change is due to a reduction in the planform area of the wing at lower values of the δ, considerably large Mach number, and a decrease in the flow deflection angle will have a different flow field on the surface of the wing.

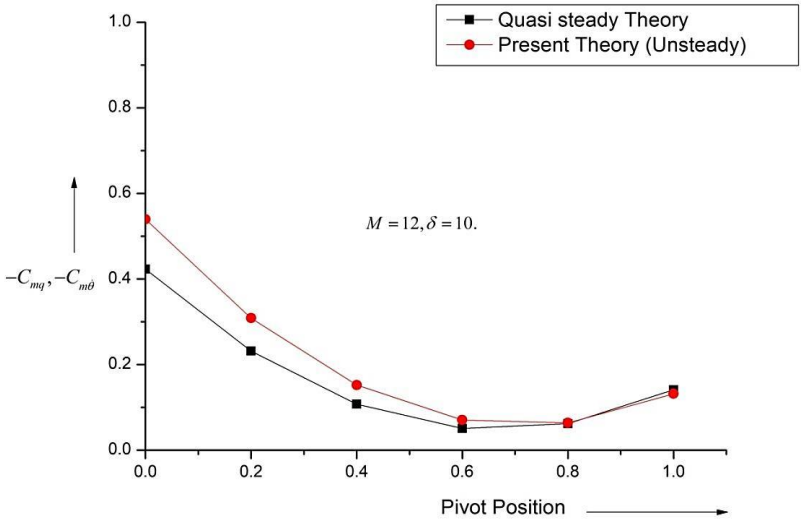

Fig.11. Unsteady and quasi-steady damping derivative with the pivot position

Figure 11 shows similar results at the more considerable value of inertia level (i.e., M = 12). The outcomes for this value of δ = 10 degrees are inline with the results obtained earlier when we compare them with δ = 20 degrees. Figure 10 shows a wide range of variations in the magnitude of the values. The discrepancies in the data are twenty-eight percent, thirty-three percent, forty-two percent, thirty-nine percent, three percent, and minus seven percent for h = 0, 0.2, 0.4, 0.6, 0.8, and 1. It is evident that for the pivot position of h= 0.8, a reversal in the trend is taking place. This implies that the numerical values of the damping derivatives, which were seen for δ = 20 degrees, have surfaced once again once the Mach number has increased considerably. It is also noticed that the damping derivatives are lower for the entire range of the pivot positions, and the outcomes are on similar lines, as was seen for δ = 20 degrees. This drastic change is due to a reduction in the planform area of the wing at lower values of the δ, and a decrease in the flow deflection angle will have a different flow field on the surface of the wing. This trend may also be attributed due to the considerable large Mach number, which also satisfies the Mach number independence principle.

ISSN: 2005-4238 IJAST

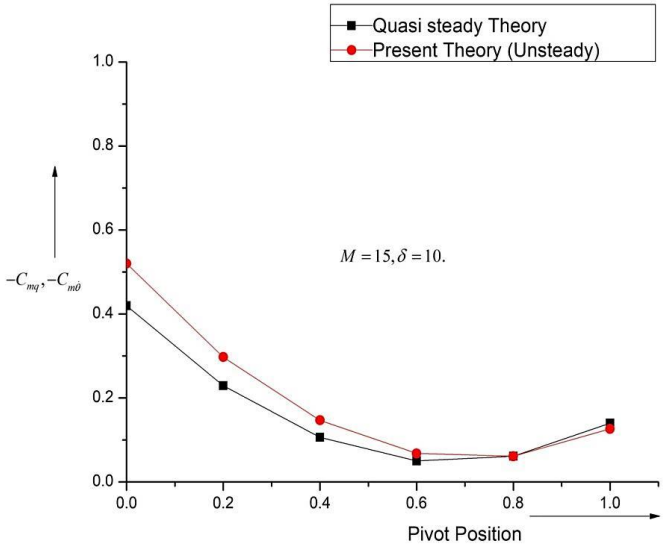

Fig. 12 Unsteady and quasi-steady damping derivative with the pivot position

Figure 12 shows similar results at the more considerable value of inertia level (i.e., M = 15). The outcomes for this value of δ = 10 degrees are inline and similar to the results obtained earlier when we compare them with δ = 20 degrees. Figure 12 shows a wide range of variations in the magnitude of the values. The discrepancies in the data are twenty-four percent, thirty percent, thirty-eight percent, thirty-five percent, minus one percent, and minus ten percent for h = 0, 0.2, 0.4, 0.6, 0.8, and 1. The reversal in trends remained at h= 0.8. This implies that the numerical values of the damping derivatives, which were seen for δ = 20 degrees, are revisiting once again once the Mach number has increased considerably. This trend may also be attributed due to the considerable large Mach number at which the pressure distribution on the surface of the wing remains unchanged as an increase in the inertia level will not result in any change as it has almost reached the steady-state.

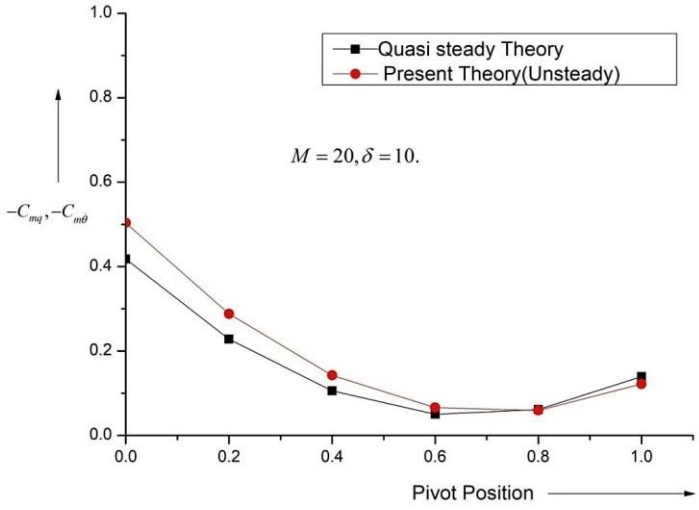

Fig. 13 Unsteady and quasi-steady damping derivative with the pivot position

ISSN: 2005-4238 IJAST

Figure13 shows the results of damping derivatives at the most considerable value of inertia level (i.e., M = 20). The outcomes for this value of δ = 10 degrees are inline and similar to the results obtained earlier when we compare them with δ = 20 degrees. The discrepancies in the data are twenty-one percent, twenty-six percent, thirty-four percent, thirty-one percent, minus three percent, and minus twelve percent for h = 0, 0.2, 0.4, 0.6, 0.8, and 1. The reversal in trends remained around h= 0.8. This trend may also be attributed due to the considerable large Mach number at which the pressure distribution on the surface of the wing remains unchanged as a further increase in the inertia level will not result in any change in the flow field on the surface of the wing as it has almost reached the steady-state.

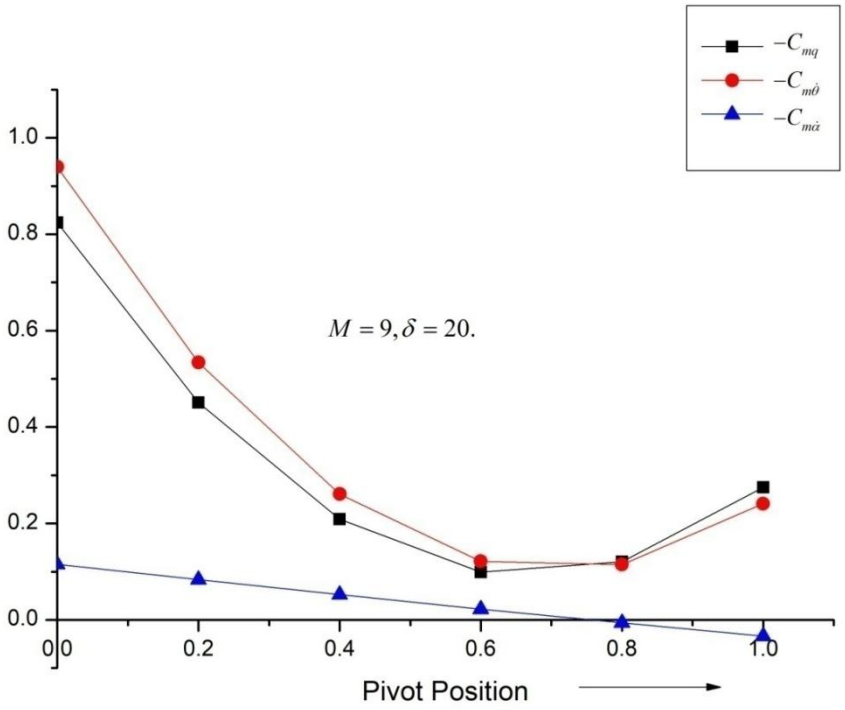

Fig. 14 Damping derivative unsteady, quasi-steady, and due to the rate of change of attack with the pivot position

Figure 14 shows results at considerable large Mach number (i.e., M = 9). This Mach number is the limiting Mach number beyond which the flow field starts becoming independent of the inertia level. The outcomes for this value of δ = 10 degrees are inline and similar to the results obtained earlier when we compare them with δ = 20 degrees. The discrepancies in the data are fourteen percent, eighteen percent, twenty-five percent, twenty-three percent, minus five percent, and minus twelve percent for h = 0, 0.2, 0.4, 0.6, 0.8, and 1. The reversal in trends is around at h = 0.7. This implies that outcomes of the damping derivatives, which were found for δ = 20 degrees, are realized once again once the Mach number has increased considerably to the limiting value. Figure 14 shows the contribution to the damping derivatives due to the rate of change of angle attack alone. This data will be beneficial during the design stage of the aircraft to quantify the contribution from the angle of attack. It is well known that there is a limit on the angle of attack for the wings. Once we cross the limiting value of the incidence angle, the lift-curve slope will start declining, and this stage is known as the stalling of the airfoil. However, we are still interested in evaluating these pieces of information to use during the landing of the aircraft. The data also will be of considerable use to design the aircraft structure. While designing the aircraft structure, there is a cap on the factor of safety as well as the take-off weight of the aircraft from the end-user.

ISSN: 2005-4238 IJAST

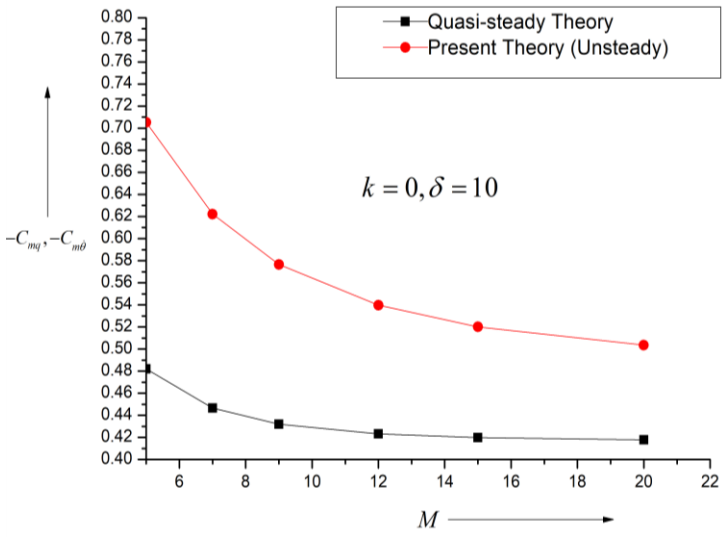

Fig. 15 Unsteady and quasi-steady damping derivative with Mach number M

Figure 15 shows the results of the stability derivatives for pivot position k = 0 and the flow deflection angles of ten degrees. When we compare the results of the damping derivatives for a fixed pivot position, the results show different trends. The results show that in the Mach number, the independence principle is attained at Mach M = 10 for quasi-steady damping derivatives. In contrast, when we see the results of unsteady flow, there is a progressive decrease in the unsteady damping derivative. The physics behind this trend may at lower values of flow deflection angles. The planform area of the wing is small, which will have different flow field on the surface of the wing. Due to this change in the surface pressure of the wing, the center of pressure also will change as it assumes different values at variable Mach numbers. The other reason for unsteady damping derivative not to reach the steady-state may be the additional component of the damping derivative, which depends on the rate of change of angle of attack. During the flight, while maneuvering the aircraft, the wing and its control surface will have a variable angle of incidence to accomplish the mission requirements.

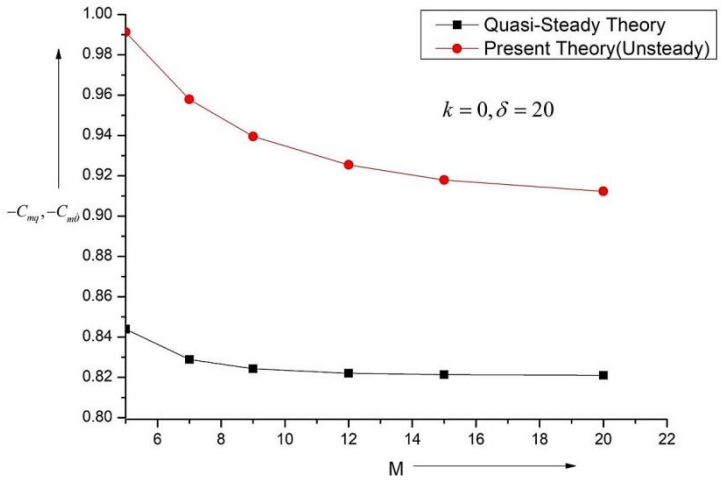

Fig. 16 Unsteady and quasi-steady damping derivative with Mach number M

ISSN: 2005-4238 IJAST

Figure 16 shows the results of the stability derivatives for pivot position k = 0 and the flow deflection angles of twenty degrees. When we compare the results of the damping derivatives for a fixed pivot position, the results show different trends. The results show that the Mach number, the independence principle, is attained earlier as compared to the previous case, which was seen at Mach M = 10 for quasi-steady damping derivatives. In contrast, when we see the results of unsteady flow, there is a progressive decrease in the unsteady damping derivative. The physics behind this trend may be for this value of flow deflection angles. The planform area of the wing is comparatively large, which will have different flow field on the surface of the wing. Due to this change in the surface pressure of the wing, the center of pressure will move downstream as it assumes different values at variable Mach numbers. The other reason for unsteady damping derivative to reach the steady-state may as compared to lower flow deflection angle may be the additional component of the damping derivative, which depends on the rate of change of angle of attack.

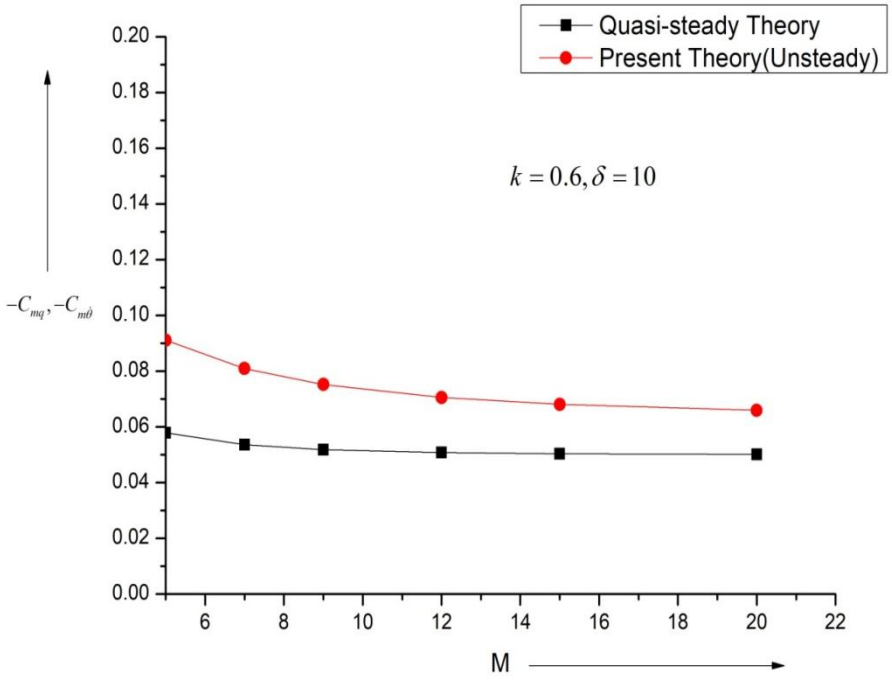

Fig.17 Unsteady and quasi-steady damping derivative with Mach number M

Results of damping derivatives for a wide range of Mach numbers at k = 0.6 for δ = 10 degrees are shown in Figure 17. It is seen that the numerical values of the damping derivatives are small. This may be due to the selection of the hinge point of the wing. For this pivot position, the center of pressure will also lie in the neighborhood of the hinge resulting in a tiny moment arm. Another reason for this trend seems to be the small-angle delta resulting in a small planform area of the wing. This little value of δ will result in minimal pressure on the wing surface, resulting in a lower normal force on the wing surface. The steady-state in the quasi-damping derivatives is attained at M = 7, which is earlier than in the case of the unsteady damping derivatives, which happens at Mach M = 12 and above.

ISSN: 2005-4238 IJAST

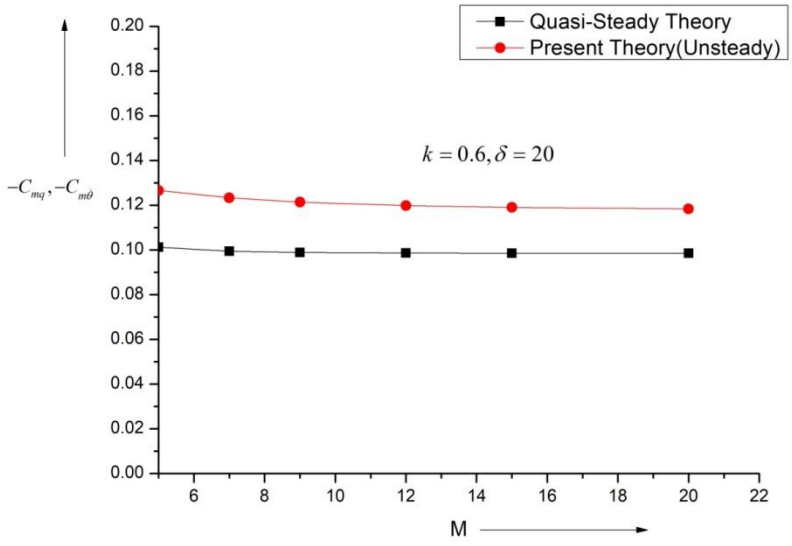

Fig. 18 Unsteady and quasi-steady damping derivative with Mach number M

Results of damping derivatives for a wide range of Mach numbers at k = 0.6 for δ = 20 degrees are shown in Figure 18. It is seen that the numerical values of the damping derivatives are marginally larger than what we got at δ = 10 degrees. This may be due to the flow deflection angle, which has changed the flow field completely. For this pivot position, the center of pressure will also lie in the neighborhood of the hinge resulting in a tiny moment arm. The steady-state in the quasi-damping derivatives is attained at M = 6, which is marginally earlier than in the case of the unsteady damping derivatives, which happens at Mach M = 8 and above. Never the less the steady-state is achieved much earlier than what was seen at lower flow deflection angles.

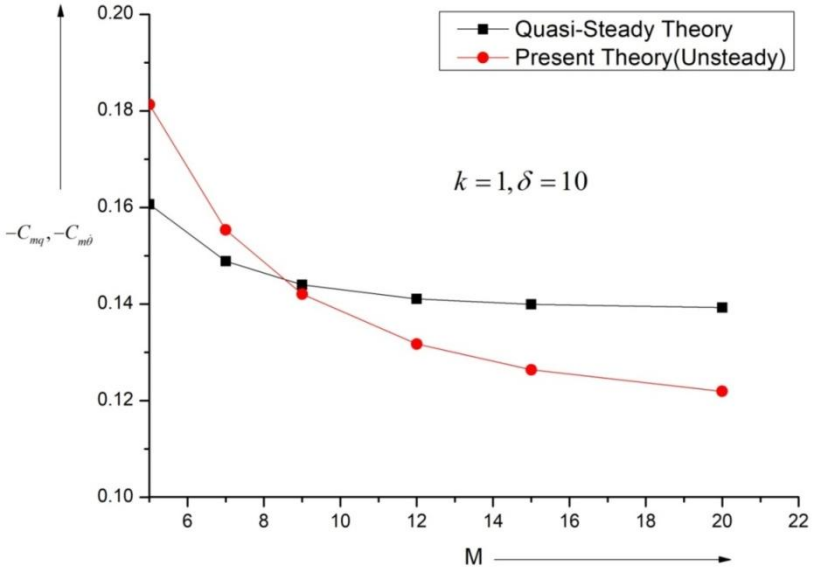

Fig. 19 Unsteady and quasi-steady damping derivative with Mach number M

ISSN: 2005-4238 IJAST

Results of damping derivatives for a wide range of Mach numbers at k = 1 for δ = 10 degrees are shown in Figure 19. It is seen that the numerical values of the damping derivatives are marginally larger than what we got at k = 0.6. This may be due to the location of the pivot position, which has changed the flow field completely. For this pivot position, the center of pressure will also lie ahead of the hinge resulting in a small moment arm. The steady-state in the quasi-damping derivatives is attained at M = 12, which is earlier than in the case of the unsteady damping derivatives, which happens at a very high Mach number M = 20 and above.

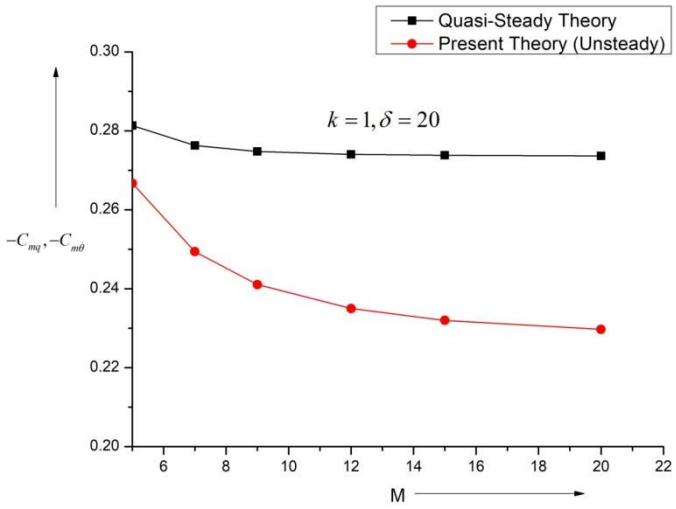

Fig. 20 Unsteady and quasi-steady damping derivative with Mach number M.

Results of damping derivatives for a wide range of Mach numbers at k = 1.0 for δ = 20 degrees are shown in Figure 20. It is seen that the numerical values of the damping derivatives are marginally larger than what we got at δ = 10 degrees. This may be due to the flow deflection angle, which has changed the flow field completely. For this pivot position, the center of pressure will also lie in the neighborhood of the hinge resulting in a tiny moment arm. The steady-state in the quasi-damping derivatives is attained at M = 7, which is much earlier than in the standard case of the unsteady damping derivatives, which happens at Mach M = 18 and above.

4. Conclusıons

Based on the above discussions, we may draw the following conclusions:

1. With the increase in Mach number, there is a progressive decrease in the damping derivatives for both the cases (i.e., unsteady and quasi-steady). The trend remained unchanged. However, with a further increase in the Mach values, the magnitude of decrease has diminished.

2. When Mach number M = 15 and above, there are no variations in the damping derivatives, and the state of steady-state is achieved. At this point, it confirms the Mach number independence principle.

3. While analyzing the results, it is seen that for pivot positions, h = 0.4 to 0.6 reversal in the trend takes place.

4. For the entire range of the Mach number, the location of the center of pressure remained unchanged

ISSN: 2005-4238 IJAST

for a fixed value of the flow deflection angle δ.

5. For the lower flow deflection angle of the wing, the magnitude of the damping derivatives is smaller as compared to the higher values of δ.

6. The contribution to the damping derivatives from the rate of change of angle of attack is around 20 percent of the quasi-steady values.

7. The numerical values of the damping derivatives for quasi-steady cases, which was lower in magnitude, becomes more considerable for the pivot position in the neighborhood of the center of pressure. Also, it shows that the damping derivatives are higher for the entire range of the pivot positions.

8. The results for flow deflection angles of ten degrees and twenty degrees show a different trend. At lower Mach numbers when the flow deflection angles of ten degrees, the unsteady damping derivatives are larger than the damping derivatives of quasi-steady for Mach M = 5, 7, and 9, when the Mach number reaches around ten and above the behavior of the damping derivatives, which was seen at flow deflection angle twenty degrees visits once again.

9. When we compare the results of the damping derivatives for a fixed pivot position, it is seen that the damping derivatives show a different trend for two different values of the flow deflection angle δ. The steady-state varies for two values of δ.

When we look at the damping derivatives at hinge point k = 0.6, the magnitude is small. The steady-state is attained early for quasi-steady in comparison to the unsteady damping derivatives.

References

1. Light Hill, M. J.,1953, "Oscillating Aerofoil at High Mach Numbers," Journal of Aeronautical Sciences, Vol. 20, June, pp.804-812.
2. Miles, J. W., 1960, "Unsteady flow at hypersonic speeds, Hypersonic Flow," Butterworth's Scientific Publications, London, pp. 185-197.
3. Ghosh, K. (1977). "A New Similitude for Aerofoils in Hypersonic Flow." Proceedings of the 6thCanadian Congress of Applied Mechanics, Vancouver, Canada, May 29-June 3, pp.685-686.
4. Ghosh K, Mistry, B. K, 1980, "Large incidence hypersonic similitude and Oscillating non-planar wedges," AIAA Journal, Vol., 18, No. 18, August, pp. 1004 -1006.
5. Ghosh K., 1984, "Hypersonic large deflection similitude for quasi-wedges and quasi cones," The Aeronautical Journal, March, pp. 70-76.
6. Ghosh, K. 1984, "Hypersonic Large Deflection Similitude for oscillating delta wings," Aeronautical Journal, Oct., pp. 357-361.
7. Ghosh K. and Vempathi, M. and Das, D. 1985, "Hypersonic flow past non-slender wedges, cones and ogives in oscillation," The Aeronautical Journal, August, pp. 247-256.
8. Ghosh K., 1986, "Unified supersonic/hypersonic similitude for oscillating wedges and plane ogives," AIAA Journal, Vol. 24, No.7, July, pp.1205-1207.
9. Hui W. H. et al., 1982, "Oscillating Supersonic/Hypersonic wings at High Incidence," AIAA Journal, Vol. 20. Issue 3, March, pp. 299-304.
10. Ghosh K, 1983, "Unified similitude for wedge and cone with attached shock," extended abstract published in Canadian Congress of Appl. Mech., University of Saskatchewan, Saskatoon, Canada, May 31- June 3, pp.533-544.
11. Asha Crasta and S. A. Khan (2015). "Effect of Angle of the attack on Stiffness derivative of an oscillating supersonic delta wing with curved leading edges." IOSR-JMCE issue1, Volume12,

December,pp12-25.
12. Khan S. A. and Asha Crasta, 2010," Oscillating Supersonic delta wings with Curved Leading Edges," Advanced Studies in Contemporary Mathematics, Vol. 20, No.3, pp. 359-372.
13. Asha Crasta and Khan S. A., 2012, "Oscillating Supersonic delta wing with Straight Leading Edges," International Journal of Computational Engineering Research, Vol. 2, Issue 5, September, pp. 1226-1233.
14. Asha Crasta and S.A., Khan, 2013, "Stability Derivatives in the Newtonian Limit," International Journal of Advanced Research in Engineering and Technology, Vol.4, Issue 7, Nov-Dec.,pp.276-289
15. Asha Crasta, S. A. Khan, 2014, "Effect of angle of incidence on roll damping derivative of a delta wing," International Journal of Emerging Trends in Engineering and developments, Vol. 2, Issue 4, March 2014, pp. 343-356.
16. Asha Crasta, S. Pavitra, and Khan S. A., 2016, "Estimation of Surface Pressure Distribution On a Delta Wing with Curved Leading Edges in Hypersonic/Supersonic Flow," International Journal of Energy, Environment and Economics, Vol. 24, Issue No.1, pp. 67-73, e-ISSN: 2349-7688.
17. Aysha Shabana, Renita S Monis, Asha Crasta and Khan S. A., 2018, "Effect of semi vertex angle on stability derivatives for an oscillating cone for a constant value of specific heat ratio," International Journal of Engineering & Technology, Vol. 7, Issue No.3, pp. 386-390.
18. Aysha Shabana, Renita S Monis, Asha Crasta and Khan S. A., 2018, "Estimation of Stability derivatives in Newtonian Limit for an oscillating cone" IOP Conf. Series Materials Science and Engineering 370 (2018) 012061 DOI:10.1088 /1757-899X/370/1/012061.
19. Aysha Shabana, Renita S Monis, Asha Crasta and Khan S. A., 2018, "Effect of semi vertex angle on stability derivatives for an oscillating cone for a constant value of specific heat ratio," International Journal of Engineering and Technology,7(3.29)(2018)386-390.
20. Aysha Shabana, Renita S Monis, Asha Crasta and Khan S. A., 2018, "The computation of Stiffness Derivative for an Ogive in Hypersonic Flow," International Journal of Mechanical and Production Engineering Research and Development(IJMPERD), Vol.8, Issue5,pp.173-184, June,2018, ISSN(online):2249-8001, ISSN(print)2249-6890.
21. Renita S Monis, Asha Crasta and Khan S. A., 2019, "An Effect of sweep angle on roll damping derivative for a delta wing with curved leading edges in the unsteady flow," International Journal of Mechanical and Production Engineering Research and Development (IJMPERD), Vol.9, Issue No.2, April 2019, pp. 361-374.
22. Renita S Monis, Asha Crasta and Khan S. A., 2019, "Evaluation of Stiffness Derivative for a delta wing with Straight leading Edges in Unsteady Flow."International Journal of Engineering and Advanced Technology (IJEAT), Vol.8, Issue No. 3S, February 2019, pp. 754-762.
23. Renita S Monis, Asha Crasta and Khan S. A., 2019, "Effect of Sweep Angle and a Half Sine Wave on Roll Damping Derivative for a delta wing." International Journal of Recent Technology and Engineering (IJRTE), ISSN:2277-10.35940/ijrte.B1184.0782S319, Vol. 8, Issue No.2S, August 2019, pp. 984-989.
24. Renita S Monis, Asha Crasta and Khan S. A., 2019, "Estimation of Damping derivatives for delta wings in Hypersonic Flow for a Straight leading edge," International Journal of Mechanical and Production Engineering Research and Development (IJMPERD), Vol.9, Issue No.5, October 2019, pp. 255-264.
25. Renita S Monis, Asha Crasta, Mohammed Faheem and Khan S. A., 2019, "Analysis of Damping Derivatives for Delta wings in Hypersonic Flow for curved Leading edges with Full SineWave."International Journal of Engineering and Advanced Technology (IJEAT), Vol.9, Issue No.1, October 2019,pp.5457-5466.
26. Renita S Monis, Asha Crasta and Khan S.A. 2020, "Analytical Estimation of Stability Derivatives of Wing with curved leading Edges at Hypersonic Mach number," Test Engineering, and Management, Vol. 83, March-April 2020, pp. 13808-13819.